

IMPORTANCE OF THE PARACELLULAR PATHWAY FOR THE TRANSPORT OF A NEW BISPHOSPHONATE USING THE HUMAN CACO-2 MONOLAYERS MODEL

XAVIER BOULENC,* ERIC MARTI,* HENRI JOYEUX,† CLAUDE ROQUES,* YVES BERGER*
and GÉRARD FABRE‡

*Sanofi Recherche and †Institut du Cancer, Montpellier, France

(Received 18 March 1993; accepted 7 July 1993)

Abstract—The transport of a new bisphosphonate, Tiludronate, was investigated on the human adenocarcinoma cell line, CACO-2. Experiments were performed 7–16 days after cells achieved confluence, conditions under which they form well-differentiated monolayers joined by tight junctions. Tiludronate transport rate across CACO-2 monolayers was independent of the temperature (4° versus 37°), of the polarity of the cell membrane (apical-to-basolateral versus basolateral-to-apical), and of the presence of metabolic poisons (sodium azide). Its transport was enhanced by either the presence of EGTA in the incubation buffer, i.e. when extracellular Ca^{2+} concentration was reduced, or by the pretreatment of monolayers with EGTA, i.e. when the intercellular spaces and the tight junctions were widened. Based on these different observations, we could suggest that Tiludronate mainly used the paracellular pathway to cross the intestinal epithelium. An increase in the Tiludronate permeability coefficient was also observed following treatment of cells with high Tiludronate concentrations, as a consequence of the direct effect of this compound on the extracellular Ca^{2+} ions. Hence, for high drug concentrations, i.e. 20 mM, we observed a decrease in free extracellular Ca^{2+} concentration, an increase in the transepithelial electrical resistance and an increase in the transport of [^{14}C]polyethyleneglycol ([^{14}C]PEG₄₀₀), a probe for the paracellular pathway. The results indicate that Tiludronate is transported across CACO-2 monolayers by the paracellular route. Moreover, it can affect its own transport by its concentration-dependent effect on tight junction widening.

Recent advances in cell and tissue culture methodologies, particularly the growth of differentiated human cells, are providing new and potentially powerful tools to investigate the transport of drug molecules across specific biological barriers. Cell systems provide the potential for rapidly evaluating the permeability of a drug, for defining the mechanisms of transport, and for testing novel strategies for enhancing drug transport [1].

The human adenocarcinoma cell lines (HT-29, T-84 and CACO-2) which reproducibly display a number of the properties of differentiated intestinal cells, have been widely used to study intestinal epithelial differentiation because of their ability to express morphological and biochemical features of adult differentiated enterocytes. As the CACO-2 cell line displays the most highly differentiated properties under standard culture conditions [2], it appears to be the most relevant *in vitro* system for investigating transepithelial transport processes [3, 4].

The CACO-2 monolayer differs from most other cell lines of the same origin in that it spontaneously differentiates into monolayer polarized enterocytes and develops characteristics of the small intestinal epithelium. Brush border hydrolase activities are similar to those reported for normal villous

enterocytes, suggesting a high level of apical differentiation [2]. CACO-2 cells grown onto collagen-coated membranes [5] form a tight monolayer of polarized epithelial cells and thus represent a potential transport model system for the small intestinal epithelium [6]. After 15 days of culture, CACO-2 cell monolayers possessed a morphology similar to that described for the simple, columnar epithelium of the small intestine. Thus, the cells appear to undergo differentiation from “crypt type cells” to “villus type cells” [2, 4].

CACO-2 monolayers have been used to evaluate different transport systems: carrier-mediated transport for phenylalanine [7, 8], taurocholic acid [9, 10], L- α -methyl dopa [11] and cephalosporins [12, 13], passive diffusion for testosterone [14] and lipophilic β -blockers [15], vasopressin analogs [16] and peptides [17, 18], and paracellular transport for hydrophilic β -blockers [19].

Correlation between oral drug absorption in humans and apparent drug permeability coefficients in the CACO-2 model has been established for different products [20]. The results obtained so far indicate that the performance of the cell models is in many cases at least as good as, and sometimes better than, many conventional drug absorption models [1, 4, 5].

Bisphosphonates are known to be poorly absorbed when given orally [21–23]. Furthermore, absorption of bisphosphonate varies extensively between and within individuals rendering difficult any accurate prediction of systemic drug concentration following

‡ Corresponding author: Dr Gérard Fabre, Sanofi Recherche, Department of Metabolism and Pharmacokinetic, 371 Rue du Professeur Blayac, 34184 Montpellier, Cédex 4, France. Tel. (33) 67.40.01.33; FAX (33) 67.75.63.21.

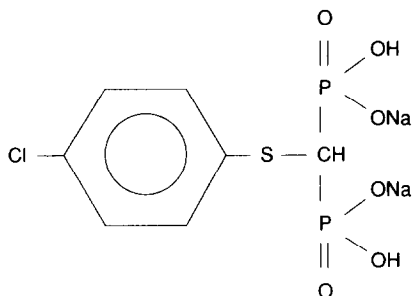


Fig. 1. Chemical structure of disodium Tiludronate.

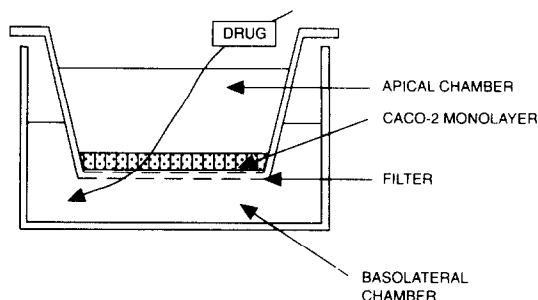


Fig. 2. Illustration of the permeable filter chambers used for transport studies. CACO-2 cells are cultured on 0.45 μ m pore collagen type I-coated inserts.

a standard dosage regimen of these compounds. The reliability of drug absorption would be enhanced and its variability reduced if absorption was increased. The purpose of this study was to use CACO-2 monolayers to evaluate the permeability of a new bisphosphonate, Tiludronate [24, 25] and to study mechanisms of its absorption under controlled conditions.

MATERIALS AND METHODS

Chemicals. 14 C-Labeled (specific radioactivity = 33 mCi/mmol) and unlabeled Tiludronate (SR 41319B) was obtained from Sanofi Recherche, Montpellier, France. Its chemical structure is illustrated in Fig. 1. [14 C]Polyethyleneglycol₄₀₀₀ ([14 C]PEG₄₀₀₀*) (M_r 4000; sp. act. = 13 mCi/g, [14 C]PEG₄₀₀; M_r 400; sp. act. = 15.3 mCi/g), and [3 H]mannitol (M_r 182; sp. act. = 30 Ci/mmol) were purchased from Amersham International (Amersham, U.K.) and New England Nuclear products (Boston, MA, U.S.A.). [14 C]Testosterone (sp. act. = 70 mCi/mmol) and [1- 14 C]glucose (sp. act. = 50 mCi/mmol) were obtained from Dositek (Orsay, France). [Ethyleneglycol-bis-(β -aminoethyl ether)- N,N,N',N' -tetraacetic acid (EGTA) was obtained from the Sigma Chemical Co. (St Louis, MO, U.S.A.).

Cell culture. CACO-2 cells, originating from a human colorectal carcinoma [26], were obtained from Dr A. Zweibaum (INSERM U-178, Villejuif, France). CACO-2 cells were grown in 75-cm² flasks at 37° in an atmosphere of 10% CO₂ using Dulbecco's modified Eagle's medium (DMEM) supplemented with 15% heat-inactivated fetal calf serum (FCS), 1% nonessential amino acids, 10 mM L-glutamine, 50 IU/mL penicillin, and 50 μ g/mL streptomycin. D-Glucose concentration in culture medium was 4.5 g/L. The medium was changed every other day until the flasks reached 90% confluence. Under these culture conditions cells became confluent 5–6 days after seeding. The cells were detached from the flasks by incubating the monolayers with trypsin [(0.25% in phosphate-buffered saline (PBS) at pH 7.4] containing 0.2% EDTA for 10 min at 37°.

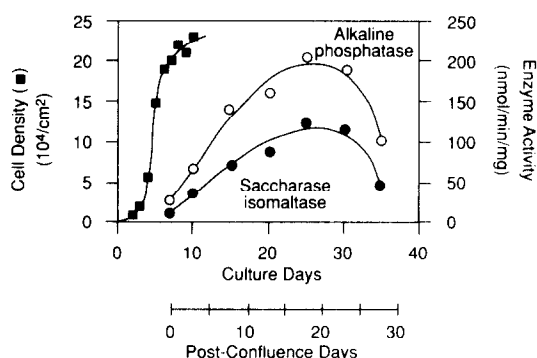


Fig. 3. Cell growth and sucrase-isomaltase and alkaline phosphatase activities in CACO-2 cells over a 20-day period. CACO-2 cells were cultured over 35 days. At specified times cells were scraped, counted on a hemacytometer and brush borders prepared. Both sucrase isomaltase and phosphatase alkaline activities are monitored as described in Materials and Methods.

All tissue culture media were obtained from EURO BIO Laboratories (Paris, France). Cells used in this study were between passage 72 and passage 88.

For transport studies CACO-2 cells were seeded onto 0.45- μ m pore collagen type I-coated inserts (Millicell-CM; pore size = 0.4 μ m; diameter = 30 mm; Millipore, Bedford, MA, U.S.A.) at 63,000 cells/cm². A basic model of the permeable filter chambers used is illustrated in Fig. 2. The monolayers used in this study were 12–20 days postseeding or 7–16 days postconfluence. A typical cell growth curve of CACO-2 cells obtained under these incubation conditions is illustrated in Fig. 3.

Integrity of the monolayers. The integrity of the monolayers was determined by measurement of the potential difference (transepithelial electrical resistance, TEER) [15, 19, 27] and by following the transepithelial transport of a macromolecular marker, PEG₄₀₀₀ [15]. The potential difference was expressed as transmembrane resistance (ohms/cm²) after subtraction of the intrinsic resistance of the

* Abbreviations: TEER, trans epithelial electrical resistance; PEG, polyethyleneglycol; FCS, fetal calf serum; PBS, phosphate-buffered saline.

model (i.e. the resistance obtained over the cell-free inserts). A monolayer with low TEER was assumed to exhibit extensive leakage through imperfect occluding junctions or holes in the monolayer [15, 19, 27]. TEER values (230 ± 50 ohms/cm²) remained constant from day 12 through day 20.

[¹⁴C]PEG₄₀₀₀ (38 µg/mL) was added to the apical side of the monolayers. The radiolabeled marker transported over CACO-2 cells was evaluated after 3 hr at 37° on a 0.5-mL aliquot part withdrawn from the basolateral chamber. The samples were measured in a liquid scintillation counter from Packard. Inserts without cells were used to determine the maximal transport of the marker during the same time period. The results were expressed as the transported percentage of the dose. The rate of [¹⁴C]PEG₄₀₀₀ transported was $0.1 \pm 0.02\%$ per hr. These results are in agreement with those previously reported by other authors [15, 19, 27] who showed that undamaged monolayers are impermeable to macromolecules such as PEG₄₀₀₀.

Preparation for transmission electron microscopic examination. The inserts were washed in PBS buffer (pH 7.2) and fixed in a solution containing 2% glutaraldehyde and 0.1 M sucrose in 0.1 M cacodylate buffer (pH 7.3) for 1 hr at 25°. The cells were rinsed in 0.1 M Hanks buffer and fixed with 1% osmium tetroxide in 0.1 M sodium cacodylate-HCl buffer for 1 hr at 25°. After dehydration, the preparation was embedded in Epon resin, sliced with a Reichert ultramicrotome, stained with uranyl acetate and lead acetate, and examined and photographed on a transmission electron microscope (Jeol 100S).

Measurement of drug transport. Drug solutions were prepared from the radiolabeled isotopes and the corresponding unlabeled compounds in Hanks buffer to give final concentrations up to 10^{-3} M. All transport experiments were performed in a 10% CO₂ incubator at 95% relative humidity and 37° in serum-free Hanks buffer (pH 7.4) containing 1 g D-glucose per liter.

The monolayers were agitated on a mixer (Red Rocker, Hoefer Scientific Instruments, San Francisco, CA, U.S.A.) at 16 rpm and a 10° angle. The radiolabeled drug solutions were added either to the apical or the basolateral side of the monolayer and aliquot parts, usually 0.2 mL, were withdrawn at previously determined intervals. Usually radiolabeled drug solutions were added to the apical compartment, except if specified, and the rate of appearance of ¹⁴C-labeled drug in the basal compartment was monitored. After withdrawing, the same volume of the buffer is added in the basal compartment to keep constant the receiver fluid volume. A maximum of four samples were taken from each chamber at regular time intervals. All inserts were checked for monolayer integrity by evaluating the TEER before each experiment and the transport of a paracellular probe after the end of the experiment.

Radioactive scintillation counting. Radioactivity was determined by liquid scintillation counting of 0.05–0.2-mL aliquot parts of the incubation medium in a Tricarb liquid scintillation spectrometer (Packard Instruments). Results were corrected to dpm by comparison with standard quench curves.

Calculations. The apparent permeability coefficient (P_{app}) was determined as previously reported [28]:

$$P_{app} = dQ/[dt \times A \times C_0]$$

where; dQ/dt is the transport rate (µg/sec) and corresponds to the slope of the regression line determined on at least four different time points, C_0 is the initial concentration in the donor chamber (µg/mL or µg/cm³), A is the area of the membrane (5.7 cm²).

HPLC analysis. The appearance of Tiludronate in the receiving chamber was also quantified following HPLC analysis, since studies from our [29] and other laboratories [30–32] recently demonstrated that CACO-2 expressed various enzymatic systems involved in both endogenous compounds and xenobiotics metabolism, such as cytochrome P450 monooxygenases, UDP-glucuronosyltransferases and glutathione-S-transferases. HPLC analyses were performed on a Varian high performance liquid chromatograph (Serie STAR 9000). UV detection was monitored at 270 nm using either a VARIAN 9050 variable wavelength detector or a Waters 990 diode array UV-visible detector. Tiludronate was separated from endogenous compounds on an Ashipak column (250 × 4.6 mm; average particle size 5 µm) from Prolabo. Elution was carried out isocratically at 1 mL/min using an acetonitrile (5%)/18 g/L Na₃PO₄-supplemented Waters Pic A buffer (95%) mixture. Retention time for Tiludronate under these HPLC conditions was around 7 min.

Treatment with a specific calcium chelator. The selective calcium chelator, EGTA, was used to bind free extracellular Ca²⁺ ions. All EGTA experiments were performed under the same conditions as the drug transport studies. The serum-free Hanks medium (containing 1.2 mM Ca²⁺) was supplemented with 2.5 mM EGTA. The medium containing EGTA was added to the two compartments, apical and basal, for periods of up to 45 min. The integrity of the monolayers was checked a few hours after the end of each experiment by the determination of [¹⁴C]PEG₄₀₀₀ transport and by the measurement of the TEER.

Determination of extracellular Ca²⁺ concentration. The concentration of Ca²⁺ ions in the incubation medium, i.e. Hanks buffer = 1.2 mM, was determined in the absence or the presence of increasing concentrations of either EGTA or Tiludronate, using an Ingold Type electrode. Calculations were determined relative to the control value.

Enzymatic activity. Brush border preparation of CACO-2 cells was performed as described previously [29]. Protein concentrations were determined by the Bio-Rad assay according to Pollard *et al.* [33] using bovine serum albumin as standard protein. Sucrase-isomaltase (EC 3.2.1.48) activity [34] and alkaline phosphatase (EC 3.1.3.1), with *p*-nitrophenyl phosphate as substrate [35], were determined as previously described.

RESULTS

Differentiation and characterization of CACO-2 cells

The index of differentiation of CACO-2 cells

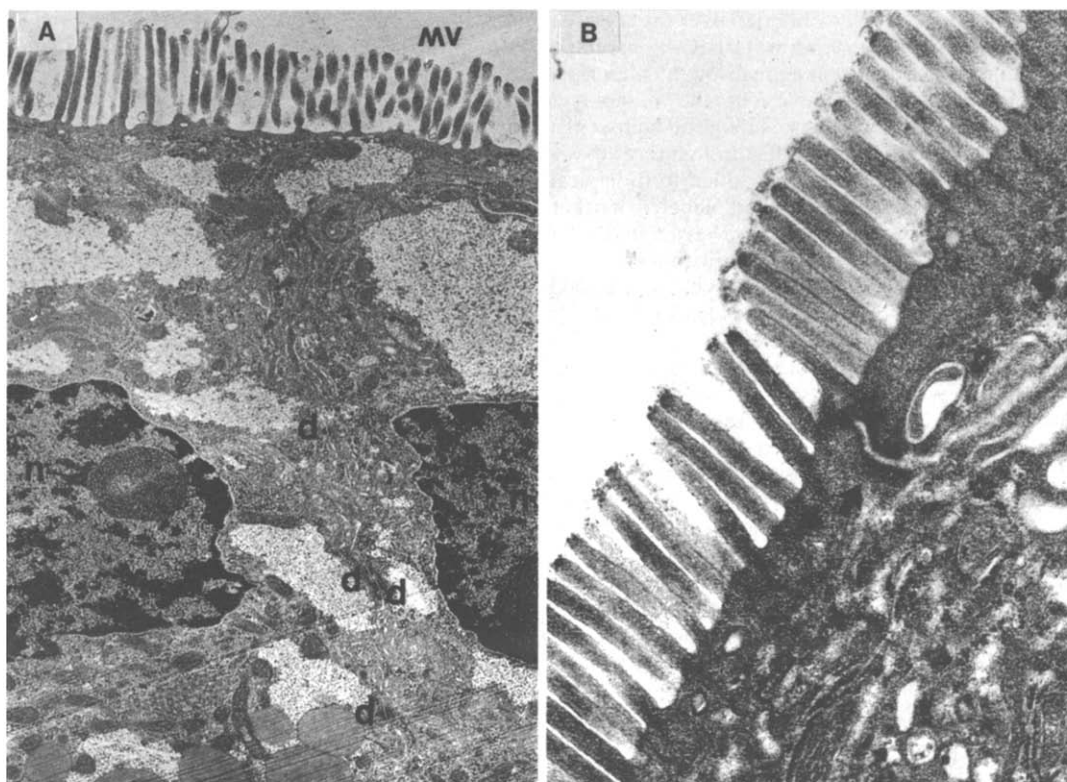


Fig. 4. Electron micrographs of CACO-2 cells. Electron micrographs of 20-day-old CACO-2 monolayers (A). The quality of desmosomes and tight junctions are illustrated in the enlargement (B). mv = microvilli; d = desmosomes; n = nuclear. The arrows indicate tight junctions.

under our incubation conditions was evaluated according to two criteria: (1) the increased expression of the marker enzymes sucrase-isomaltase and alkaline phosphatase, two enzymes present at the level of microvilli, and (2) the morphological aspect of the cells by electronic microscopy.

The biochemical parameters achieved after various periods of time in culture are shown in Fig. 3. From these data it was obvious that the differentiation process, characterized by the expression of saccharase isomaltase and alkaline phosphatase, occurred continuously from day 8 up to day 30, which corresponds to day 1 up to day 23 after cells achieved the stationary phase of growth. The values obtained were similar to those reported in the literature by others [36–39]. An electron micrograph of CACO-2 cells on postconfluence day 20 is illustrated in Fig. 4. Cells appeared cuboidal with a large distribution of mature microvilli on the apical surface, constituting a brush border membrane. We also observed desmosomes and occluding junctions (tight junctions) limited to the apical surface of the cells. These different observations confirmed that after monolayers have achieved the stationary phase of growth, CACO-2 cells spontaneously differentiated and resemble both structurally and functionally the small intestinal epithelium.

Transport of Tiludronate across CACO-2 monolayers

(a) Solubility of Tiludronate. Octanol–water

distribution determination showed that Tiludronate was highly water-soluble. Under our incubation conditions, i.e. up to 50 mM Tiludronate, more than 99% of [^{14}C]Tiludronate was recovered in the aqueous phase. Although Tiludronate, as other bisphosphonates, was reported to form polynuclear complexes with Ca^{2+} ions [40], we did not observe any increase in Tiludronate (1 mM) solubility when EGTA (2.5 mM) was added in the incubation medium.

(b) Ca^{2+} ions chelation. The effects of both EGTA and Tiludronate on extracellular free Ca^{2+} ions was investigated. The concentration of extracellular Ca^{2+} ions in Hanks medium was evaluated in the absence or the presence of increasing EGTA or Tiludronate concentrations ranging between 0.15 and 25 mM. A 50% complexation of Ca^{2+} ions was achieved for EGTA and Tiludronate concentrations around 0.5 and 20 mM, respectively. These data confirmed previous observations from Bonneri *et al.* [40]. In the following experiments, Tiludronate concentration was set at 1 mM, conditions under which free extracellular Ca^{2+} concentration was not affected.

(c) Tiludronate transport. The permeability coefficient for Tiludronate transport was evaluated following addition of 1 mM Tiludronate in the apical compartment. The permeability coefficient was determined to be $4.0 \times 10^{-7} \pm 2.2 \times 10^{-7}$ cm/sec ($N = 8$), based on experiments performed on

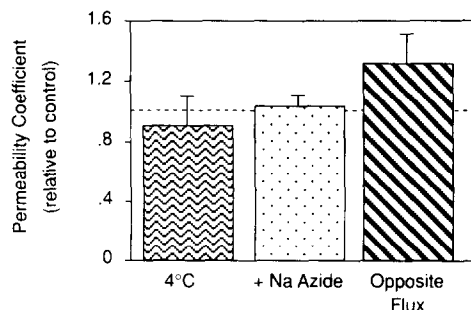


Fig. 5. Effects of sodium azide and low temperature on Tiludronate transport. Tiludronate (1 mM) was added in the apical compartment of CACO-2 monolayers and permeability coefficients were determined either at 37°, at 4° or in the presence of sodium azide. The permeability coefficient was also determined following addition of Tiludronate (1 mM) in the basal compartment and measurement of the radiolabel in the apical compartment (opposite flux). Results are expressed as the mean \pm SEM of four different inserts run in the same experiment. When experiments were performed on separate days, results are reported relative to their own control run simultaneously.

different cell preparations and on 10–16 days postconfluence cells. Similar results were obtained when quantification was performed following HPLC analysis (data not shown). The apparent large inter-experiment variability was mostly due to the fact that Tiludronate transport was relatively low due to its type of transport (discussed further in the following paragraphs). The effect of the aqueous boundary layer on Tiludronate transport was also investigated. No increase nor decrease of Tiludronate transport was observed when the angular rotation was increased from 16 to 150 rpm. However, under the same conditions, testosterone permeability coefficient increased from approximately 50 to 290×10^{-6} cm/sec (data not shown).

(d) *Effects of sodium azide and low temperature on Tiludronate transport.* The permeability coefficient of Tiludronate was also evaluated in the “basal-to-apical” direction. The transport rate of Tiludronate appeared to be not statistically different in either the “basal-to-apical” or in the “apical-to-basal” direction, i.e. the opposite flux. Likewise, no effect was observed when incubation was performed at 4° (Fig. 5). The effect of sodium azide, an energy poison, was examined on the permeability coefficient of Tiludronate across the CACO-2 monolayers. The presence of 1.0 mM sodium azide in the apical compartment has no effect on Tiludronate transport, as illustrated in Fig. 5.

(e) *Effect of calcium-chelator treatment of CACO-2 cells on Tiludronate transport.* In the following experiments, the selective calcium-chelator EGTA, at an extracellular concentration of 2.5 mM, was used to bind free extracellular Ca^{2+} ions. Previous studies performed by Artursson and Magnusson [19] on the CACO-2 cell model had already showed that the minimal effective concentration of EGTA on the transmembrane resistance was 2.5 mM for a

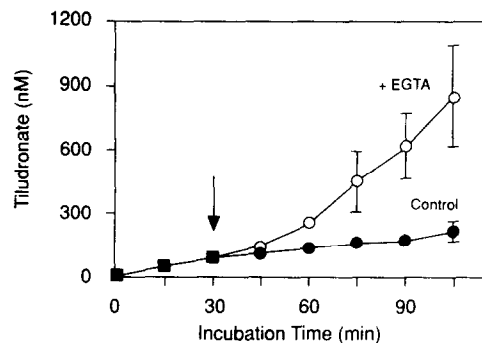


Fig. 6. Effect of EGTA co-incubation on Tiludronate transport. [^{14}C]Tiludronate (1 mM final concentration) was added to the apical side of CACO-2 cells and its appearance in the receiving chamber was monitored (■). At the time indicated by the arrow, EGTA (2.5 mM final concentration) was added and the [^{14}C]Tiludronate appearance was determined in the absence (●) or the presence (○) of EGTA. Results are expressed as the mean \pm SEM of three different inserts run in the same experiment.

maximal exposure of 45 min. Under these incubation conditions, TEER decreased from 253 ± 7 ohm \times cm 2 to 147 ± 3 ohm \times cm 2 . The transmembrane resistance was completely restored after a 2-hr incubation period at 37°, EGTA-treated cells being indistinguishable from control monolayers (data not shown).

Tiludronate (1 mM final concentration) was added to the apical side of the cells and its appearance in the receiving chamber was monitored as a function of time over 2 hr. After 30 min, EGTA (2.5 mM final concentration; 200 μL of a 25 mM pH adjusted-EGTA solution containing 1 mM Tiludronate) was added on the apical side of the cells and its influence on Tiludronate transport was evaluated. Results are illustrated in Fig. 6. Following addition of EGTA, a time-dependent increase in drug transport was observed over the first 30 min of co-incubation, a maximal rate of Tiludronate transport being achieved after 45 min. In EGTA-treated CACO-2 monolayers, we observed a 7.7-fold increase in drug transport compared to control monolayers.

A clear effect of the reduction of the extracellular Ca^{2+} concentration was observed for the hydrophilic drug, Tiludronate, as illustrated in Fig. 7. The transport of the latter was evaluated after a 30-min exposure to the low Ca^{2+} medium, i.e. in the presence of 2.5 mM EGTA (conditions under which extracellular Ca^{2+} ions are chelated and tight junctions widened). Then EGTA-containing medium is removed and 37°-fresh medium added. A 6.6-fold increase in Tiludronate transport was observed during the subsequent 30 min period. This increase in permeability was reversible since the transport rate returned to normal levels after a 4-hr recovery period in EGTA-free medium at 37°. Similar experiments were also performed with testosterone, a lipophilic endogenous compound which is known to be passively transported across CACO-2 cells. The reversible opening of the junctional complex

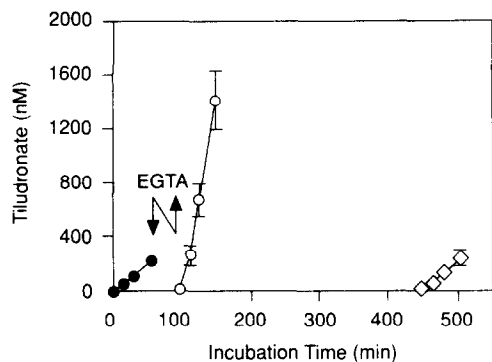


Fig. 7. Effect of EGTA-pretreatment of CACO-2 cells on Tiludronate transport. The transport of [^{14}C]Tiludronate (1 mM final concentration) over CACO-2 monolayers was measured before (●), immediately after (○) and 5 hr after (◇) a 45-min treatment of cells with 2.5 mM EGTA. Results are expressed as the mean \pm SEM of three different inserts. The same monolayers were used in all three experiments.

had no effect on the transport rate of testosterone ($18.0 \times 10^{-6} \pm 2.7 \times 10^{-6}$ cm/sec versus $18.8 \times 10^{-6} \pm 1.8 \times 10^{-6}$ cm/sec before and after the 45-min pretreatment of monolayers with EGTA, respectively).

For a better understanding of Tiludronate transport across CACO-2 monolayers, we compared the effect of EGTA on the permeability coefficient of Tiludronate and mannitol which has already been described as a marker of the paracellular transport in this epithelial model [1]. The permeability coefficients for both mannitol and Tiludronate were similar at $3.50 \times 10^{-7} \pm 0.15 \times 10^{-7}$ cm/sec and $3.3 \times 10^{-7} \pm 0.6 \times 10^{-7}$ cm/sec (SEM; $N = 3$), respectively and were affected in a similar manner by the presence of 2.5 mM EDTA, $26.5 \times 10^{-7} \pm 0.3 \times 10^{-7}$ cm/sec and $23.1 \times 10^{-7} \pm 3.2 \times 10^{-7}$ cm/sec for mannitol and Tiludronate, respectively.

Effect of Tiludronate on the paracellular pathway

(a) *Effect on monolayer morphological aspect.* Examination of untreated 15-day postconfluence CACO-2 monolayers by scanning electron micrography did not reveal any discernible gaps or holes in the monolayer, in the shape and the density of microvilli or in the quality of the desmosomes and the tight junctions (Fig. 8). When CACO-2 monolayers were incubated for 30 min with either 2.5 mM EGTA or 30 mM Tiludronate, the normal polygonal shape of the untreated CACO-2 cells was lost and cells appeared contracted and rounded. This suggests a common effect of both EGTA and Tiludronate at the level of the monolayers, although occurring at a 10-fold higher concentration for Tiludronate compared to EGTA.

(b) *Effect on TEER.* The effect of Tiludronate on TEER was evaluated following addition of 1 or 50 mM Tiludronate in the apical compartment. TEER values of 10-day postconfluence monolayers

were $224 \pm 10 \text{ ohm} \times \text{cm}^2$ (Fig. 9). Following treatment of CACO-2 monolayers with Tiludronate, we observed a time-related decrease in the TEER, achieving a plateau value at $174 \pm 8 \text{ ohm} \times \text{cm}^2$ and $88 \pm 3 \text{ ohm} \times \text{cm}^2$, 40 min after addition of 1 and 50 mM Tiludronate, respectively. Under the latter conditions, i.e. a 40-min exposure to 50 mM Tiludronate, the TEER was almost completely restored after a recovery period of 30 min, $202 \pm 26 \text{ ohm} \times \text{cm}^2$ ($N = 3$) in untreated cells versus $175 \pm 18 \text{ ohm} \times \text{cm}^2$ ($N = 3$) in Tiludronate-treated cells. This Tiludronate-mediated decrease in TEER was similar to that observed following a 45-min pretreatment of CACO-2 cells with 2.5 mM EGTA.

(c) *Effect on PEG₄₀₀ paracellular transport.* PEG₄₀₀, a marker for paracellular transport, has been intensively used to evaluate the permeability of the CACO-2 cell monolayers. The filters containing 15-day postconfluence CACO-2 cells were essentially impermeable to the test compound. A coefficient of permeability of $6 \times 10^{-7} \pm 0.3 \times 10^{-7}$ cm/sec was achieved for CACO-2 cells of postconfluence day 10 to day 20. [^{14}C]PEG₄₀₀ flux across the monolayer was increased up to $60 \times 10^{-7} \pm 10 \times 10^{-7}$ cm/sec when 15 mM Tiludronate was added in the apical compartment. In a similar manner, the permeability coefficient for PEG₄₀₀ was $330 \times 10^{-7} \pm 9 \times 10^{-7}$ cm/sec following addition of 2.5 mM EGTA (Fig. 10).

This increase in PEG₄₀₀ flux for Tiludronate concentrations exceeding 5 mM could be attributed either to an opening of tight junctions by Tiludronate, a consequence of the binding of free extracellular Ca^{2+} ions or to a cytotoxicity occurring at high non-physiological Tiludronate concentrations. This hypothetical cytotoxic effect of Tiludronate was investigated by evaluating both membrane integrity (Trypan blue dye exclusion) and the ability of monolayers to transport different markers such as testosterone, which cross the cells by passive diffusion, and glucose which is actively transported by CACO-2 cells. Glucose transport was determined at a single drug concentration, i.e. 1 mM and over a 60-min period. As reported in Table 1, characteristics of CACO-2 cells remained similar before or after 1-hr exposure to a high Tiludronate concentration, in terms of both cell viability and probes transport. Moreover we demonstrated that 6 hr following a 60-min treatment of CACO-2 cells with 50 mM Tiludronate, CACO-2 cells with 50 mM Tiludronate, TEER values remained similar to those obtained before Tiludronate treatment (data not shown).

(d) *Effect of Tiludronate on [^{14}C]Tiludronate transport.* The Tiludronate transport rate across CACO-2 cells was investigated over 60 min following addition of either 1 or 20 mM [^{14}C]Tiludronate in the apical compartment, after which the permeability coefficients for Tiludronate transport were evaluated. When Tiludronate concentration was increased from 1 to 20 mM, we observed first a steady state in Tiludronate permeability coefficient around $5.0 \times 10^{-7} \pm 1.2 \times 10^{-7}$ cm/sec up to a 5 mM concentration, and then a concentration-related increase in the permeability coefficient to achieve

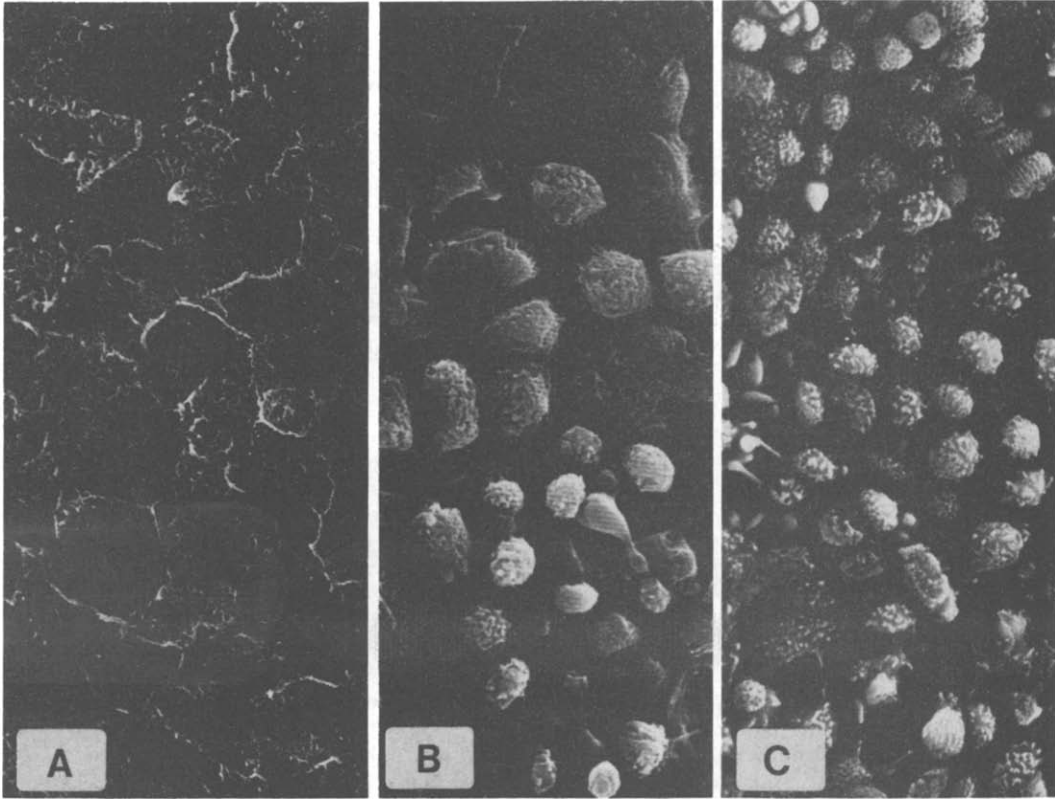


Fig. 8. Scanning electron micrographs showing the surface of the CACO-2 cell monolayers. Postconfluence 10-day CACO-2 cells were incubated for 30 min in the absence (A) or the presence of either 2.5 mM EGTA (B) or 50 mM Tiludronate (C) and scanning electron micrographs are performed. The cracks are artefacts from the preparation of the specimens.

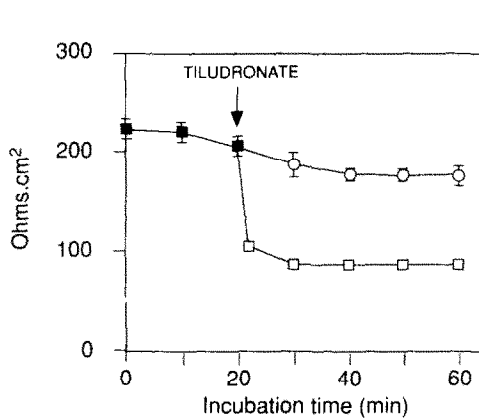


Fig. 9. Effect of Tiludronate on TEER of CACO-2 monolayers. TEER was evaluated on 7-day postconfluence cells before (■) or after addition of 1 mM (○) or 50 mM (□) Tiludronate in the apical compartment of CACO-2 monolayers. Results are the mean \pm SEM of four different inserts run in the same experiment.

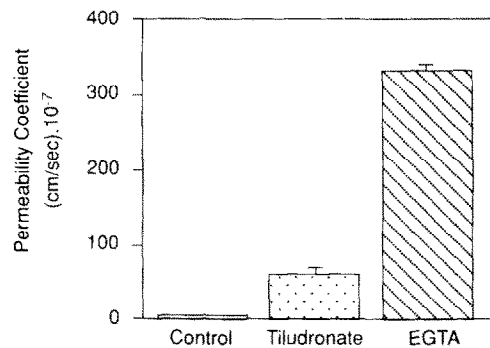


Fig. 10. Effect of Tiludronate and EGTA on PEG₄₀₀ flux across CACO-2 monolayers. Fifteen to twenty day postconfluence CACO-2 monolayers were incubated over 1 hr with [¹⁴C]PEG₄₀₀ in the absence or the presence of either 2.5 mM EGTA or 15 mM Tiludronate. [¹⁴C]PEG₄₀₀ flux across the cell membrane was monitored and the permeability coefficient of PEG₄₀₀ determined every 15 min over 90 min. Results are the mean of three different inserts performed in a single experiment.

Table 1. Cytotoxic effect of Tiludronate on CACO-2 cells

	Untreated cells	Tiludronate-treated cells
Cell viability		
Trypan blue dye exclusion (%)	94 \pm 2	93 \pm 3
Protein recovery (mg/10 ⁶ cells)	2.3 \pm 0.5	2.1 \pm 0.3
Permeability coefficient		
Testosterone; (cm/sec) $\times 10^{-5}$	7.4 \pm 0.5	8.6 \pm 0.2
Glucose*; (cm/sec) $\times 10^{-5}$	6.1 \pm 1.3	6.8 \pm 1.2

CACO-2 cells were incubated for 1 hr with 50 mM Tiludronate and different cell characteristics were determined.

* Determined at a single glucose concentration, i.e. 1 mM.

$20.0 \times 10^{-7} \pm 4.6 \times 10^{-7}$ cm/sec at 20 mM Tiludronate.

DISCUSSION

The human intestinal epithelial cell line, CACO-2, provides a cellular model to study the differentiated functions of intestinal enterocytes. CACO-2 cells spontaneously differentiate in culture to polar cells possessing microvilli and enterocytic properties. Confluent monolayers form tight junctions between cells; thus monolayers exhibited the electrical properties characteristic of an intestinal epithelium. The region of the normal human GI tract represented by the CACO-2 model is still under investigation. While the presence of brush border hydrolases and transport pathways for bile acids and cobalamin are properties of the distal ileum, the electrical properties are more indicative of a colonic epithelium [1, 10, 20].

CACO-2 monolayers are being widely used to study the transepithelial transport pathways which differ in basic properties such as specificity, saturability, competitiveness, unidirectionality etc. CACO-2 cells were demonstrated to actively transport L- α -methyl dopa [11]. Active carriers have been shown to be time, pH, concentration, glucose and temperature dependent. Furthermore, this kind of transport was inhibited by neutral as well as basic amino acids and by metabolic inhibitors. CACO-2 monolayers have recently been used to investigate the active transport of ions and different endogenous products, such as bile acids, vitamins and amino acids, over the intestinal epithelium. Saturation kinetics are generally an indication that the transport is not via passive diffusion. Hence, Hu and Borchardt [11] demonstrated that the permeability of L- α -methyl dopa, which uses a transcellular transport, was disproportionately higher at 1 mM than at a higher concentration, i.e. 2.5 mM.

However, since most drugs are transported over the intestinal epithelium by passive diffusion, the CACO-2 model was investigated for its usefulness in studying the passive diffusion of various drugs such as β -adrenoceptor antagonists. β -Blockers were transported by passive diffusion over the CACO-2 cells [15]. The transport was therefore not saturable and the transport rate from the luminal to the

basolateral side of the monolayer was the same as that in the opposite direction. The epithelial monolayer is comprised of the lipophilic cell membranes and the intercellular junctions between the cells. The intercellular spaces are sealed by tight junctions which reduce their pore radius to a few Ångström units [41]. The contribution of this paracellular pathway to the total permeability of the epithelial monolayer is only significant for drugs that are transported slowly across the cell membrane, e.g. hydrophilic compounds with a low molecular mass and very low partition coefficients [20].

The intestinal absorption of various bisphosphonates i.e. 1-hydroxyethylidene-1,1-bisphosphonate (HEBP) and dichloromethylene bisphosphonate (Cl₂MBP), has already been shown [22, 23] to be low and in the order of a few per cent in humans. Furthermore, their absorption varied both between individuals and within the same individual, making accurate oral dosage of these compounds difficult [21–23]. Based on the observation that bisphosphonates formed polynuclear complexes with calcium [21, 22] and were precipitated as calcium-bisphosphonates, Janner *et al.* [21] investigated whether the calcium chelator EDTA could improve intestinal absorption of different bisphosphonates, including Cl₂MBP, in the rat. Indeed, EDTA did increase the absorption of these bisphosphonates but only at certain doses of these compounds and at high EDTA concentrations, making this chelator unsuitable for clinical use. Among various explanations for this increase in bisphosphonate availability, they suggested that EDTA could directly enhance intestinal permeability, a consequence of the reversible decrease in the calcium and magnesium content of the intestinal epithelium associated with ultrastructural alterations at the level of tight junctions. EDTA has also been described as enhancing the intestinal absorption of drugs such as heparin and synthetic heparinoids by increasing their intestinal permeability [42].

In this study, we demonstrated the paracellular transport of Tiludronate, a new bisphosphonate, across CACO-2 monolayers. The transport of Tiludronate was relatively slow, independent of the temperature (4° versus 37°), of the polarity of the cell membrane (apical-to-basolateral versus

basolateral-to-apical), of the absence or presence of a metabolic inhibitor (sodium azide), but highly dependent of EGTA, a calcium chelator which reduces the extracellular calcium concentration, i.e. conditions under which the intercellular spaces were widened and the tight junctions were resolved at the ultrastructural level. This increase in Tiludronate transport following EGTA-treatment, was preserved for only a few hours after EGTA removal, consistent with its reversal effect on tight junction widening. This is in agreement with different findings which show that hydrophilic drugs with a low lipid solubility are transported at a slow rate across the cell membrane. Under these conditions, when the transcellular transport rate is reduced, the transport through the alternative paracellular route becomes more marked.

When CACO-2 cells were exposed to increasing Tiludronate concentrations of up to 20 mM, we observed (i) a decrease in the TEER, (ii) an increase in the transmembrane transport of mannitol (data not shown) and PEG₄₀₀, two probes of the paracellular component, and (iii) an increase in the permeability coefficient of Tiludronate. These different phenomena could be the consequence of either an indirect effect of Tiludronate on tight junction regulation, by decreasing free Ca²⁺ ions, or a cytotoxic effect on CACO-2 cells. Although an effect of Tiludronate on membrane characteristics could not be completely excluded, we demonstrated that CACO-2 cells exposed for 3 hr with 50 mM Tiludronate did not accumulate Trypan blue dye, a marker of cellular integrity, nor did they exhibit any change in the passive diffusion of testosterone [14] or in the active transport of glucose. This is in agreement with previous studies of Van Hoogdalem *et al.* [43] who reported that, due to its calcium binding properties, 3-amino-1-hydroxypropylidene-1,1-diphosphonate could be a potential paracellular absorption promoting agent. These studies suggest that following treatment of patients with Tiludronate, the drug could increase its own transport across the intestine wall and hence increase its bioavailability. These observations could explain the non linear pharmacokinetics of Tiludronate in healthy volunteers receiving increasing dosages of Tiludronate [24, 25, 44]. Although studies on many other drugs and comparison with their percentage of absorption *in vivo* will be required to determine how far one can extrapolate from the *in vitro* system to the whole animal or to man, the current results indicate that the cell culture system provides a convenient model for characterizing transport systems and measuring transport rates across an isolated human cell barrier.

Acknowledgements—The authors wish to acknowledge Dr Alain Zweibaum from INSERM U-178, Villejuif, France, for helpful scientific discussion, and Mr Max Bessoles for the quality of cell micrographs.

REFERENCES

1. Artursson P, Cell culture as model for drug absorption across the intestinal mucosa. *Crit Rev Ther Drug Carrier System* 8: 305–330, 1991.
2. Pinto M, Robine-Leon S, Appay MD, Redinger M, Triadou N, Dussaux E, Lacroix B, Simon-Assmann P, Haffen K, Fogh J and Zweibaum A, Enterocyte-like differentiation and polarization of the human colon carcinoma cell line Caco-2 in culture. *Biol Cell* 47: 323–330, 1983.
3. Zweibaum A, Differentiation of human colon cancer cells. *Life Sci* 218: 27–37, 1991.
4. Wilson G, Growth and characterization of cell and tissue cultures for the study of drug transport. *Life Sci* 218: 15–25, 1991.
5. Borchardt RT, Hidalgo IJ, Hiigren KM and Hu M, Pharmaceutical applications of cell culture: an overview. *Life Sci* 218: 1–14, 1991.
6. Hidalgo IJ, Raub TJ and Borchardt RT, Characterization of the human colon carcinoma cell line (Caco-2) as a model system for intestinal epithelial permeability. *Gastroenterology* 96: 736–749, 1989.
7. Hidalgo IJ and Borchardt RT, Amino acid transport in a novel model system of the intestinal epithelium (Caco-2) (abstract). *Pharm Res* 5: S110, 1988.
8. Hu MH and Borchardt RT, Effect of pH and glucose on L-phenylalanine transport across an intestinal epithelial cell model system (Caco-2) (abstract). *Pharm Res* 6: 589, 1989.
9. Wilson G, Hassan IF, Dix CJ, Williamson I, Shah R, Mackay M and Artursson P, Transport and permeability properties of human Caco-2 cells: an *in vitro* model of the intestinal epithelial cell barrier. *J Controlled Release* 11: 25–40, 1990.
10. Hidalgo IJ and Borchardt RT, Transport of bile acids in a human intestine epithelial cell line, Caco-2. *Biochim Biophys Acta* 1035: 97–103, 1990.
11. Hu M and Borchardt RT, Mechanism of L- α -methyldopa transport through a monolayer of polarized human intestinal epithelial cells (Caco-2). *Pharm Res* 7: 1313–1319, 1990.
12. Dantzig AH and Bergin L, Uptake of cephalosporin, cephalixin, by a dipeptide transport carrier in the human intestinal cell line, Caco-2. *Biochim Biophys Acta* 1027: 211–217, 1990.
13. Inui KI, Yamamoto M and Saito H, Transepithelial transport of oral cephalosporins by monolayers of intestinal epithelial cell line, Caco-2. *J Pharm Exp Ther* 261: 195–201, 1992.
14. Hilgers AR, Conradi RA and Burton PS, Caco-2 cell monolayers as a model for drug transport across the intestinal mucosa. *Pharm Res* 7: 902–910, 1990.
15. Artursson P, Epithelial transport of drugs in cell culture. I: A model for studying the passive diffusion of drugs over intestinal absorptive (Caco-2) cells. *J Pharm Sci* 79: 476–482, 1990.
16. Lundin S and Artursson P, Absorption of a vasopressin analogue, 1-deamino-8-D-arginine-vasopressin (dD-AVP), in a human intestinal epithelial cell line, Caco-2. *Int J Pharm* 64: 181–186, 1990.
17. Conradi RA, Hilgers AR, Ho NFH and Burton PS, The influence of peptide structure on transport across Caco-2 cells. *Pharm Res* 8: 1453–1460, 1991.
18. Burton PS, Conradi RA, Hilgers AR, Ho NFH and Maggiora LL, The relationship between peptide structure and transport across epithelial cell monolayers. *J Controlled Release* 19: 87–98, 1992.
19. Artursson P and Magnusson C, Epithelial transport of drugs in cell culture. II. Effect of extracellular calcium concentration on the paracellular transport of drugs of different lipophilicities across monolayers of intestinal epithelial (Caco-2) cells. *J Pharm Sci* 79: 595–600, 1990.
20. Artursson P and Karlsson J, Correlation between oral drug absorption in humans and apparent drug permeation coefficients in human intestinal epithelial (Caco-2) cells. *Biochem Biophys Res Commun* 175: 880–885, 1991.
21. Janner M, Mühlbauer RC and Fleisch H, Sodium EDTA

- enhances intestinal absorption of two bisphosphonates. *Calcif Tissue Int* **49**: 280–283, 1991.
22. Lamson ML, Fox JL and Huguchi WI, Calcium and 1-hydroxyethylidene-1,1'-bisphosphonic acid: polynuclear complex formation in the physiological range of pH. *Int J Pharm* **21**: 143–154, 1984.
 23. Fogelman I, Smith L, Mazess R, Wilson MA and Bevan JA, Absorption of oral diphosphonate in normal subjects. *Clin Endocrinol* **24**: 57–62, 1986.
 24. Arnoux P, Assouline C, Verschuere B, Guyonnet J, Berger Y and Cano JP, Pharmacokinetics of (4-chlorophenyl)thiomethylene bisphosphonate acid, a new bisphosphonate, in monkey. *Calcif Tissue Int* **44** (Suppl): S102, 1989 (Abstract).
 25. Necciari J, Kieffer G and Maillard D, Pharmacokinetics of (4-chlorophenyl)thiomethylene bisphosphonic acid after single and repeated administrations in healthy volunteers. *Calcif Tissue Int* **44** (Suppl): S107, 1989 (Abstract).
 26. Fogh J, Fogh JM and Orfeo T, 127 Cultured human colon cell lines producing tumors in nude mice. *J Natl Acad Sci USA* **59**: 221–226, 1977.
 27. Hidalgo IJ, Raub TJ and Borchardt RT, Characterization of the human colon carcinoma cell line (Caco-2) as a model system for intestinal epithelial permeability. *Gastroenterology* **96**: 736–749, 1989.
 28. Cruickshand JM, The clinical importance of cardioselectivity and lipophilicity in beta blockers. *Am Heart J* **100**: 160–178, 1980.
 29. Boulenc X, Bourrié M, Fabre I, Roque C, Joyeux H, Berger Y and Fabre G, Regulation of cytochrome P450IA1 expression in a human intestinal cell line, Caco-2. *J Pharm Exp Ther* **263**: 1471–1478, 1992.
 30. Peters WHM and Roelofs HJM, Time-dependent activity and expression of glutathione S-transferases in the human colon adenocarcinoma cell line Caco-2. *Biochem J* **264**: 613–616, 1989.
 31. Baranczyk-Kuzma A, Garren JA, Hidalgo IJ and Borchardt R, Substrate specificity and some properties of phenol sulfotransferase from human intestinal Caco-2 cells. *Life Sci* **49**: 1197–1206, 1991.
 32. Bjorge S, Hamelekle KL, Haman R, Rose SE, Turluck DA and Wright DS, Evidence for glucuronide conjugation of *p*-nitrophenol in the Caco-2 cell model. *Pharm Res* **8**: 1441–1443, 1991.
 33. Pollard HB, Menard R, Brandt HA, Pazoles CJ, Creutz CE and Ramu A, Application of Bradford's protein assay to adrenal gland subcellular fractions. *Anal Biochem* **86**: 761–763, 1978.
 34. Messer M and Dahlqvist A, A one step ultramicromethod for the assay of intestinal disaccharidases. *Anal Biochem* **14**: 376–392, 1966.
 35. Garen A and Levinthal C, A fine structure genetic and chemical study of the enzyme alkaline phosphatase of *E. coli*. I. Purification and characterisation of alkaline phosphatase. *Biochim Biophys Acta* **38**: 470–483, 1960.
 36. Rousset M, Laburthe M, Pinto M, Chevalier G, Rouyer-Fessard C, Dussaulx E, Trugnan G, Boige N, Brun JL and Zweibaum A, Enterocytic differentiation and glucose utilization in the human colon tumor cell line Caco-2: modulation by forskolin. *J Cell Physiol* **123**: 377–385, 1985.
 37. Zweibaum A, Triadov N, Keding M, Augeron C, Robine-Leon S, Pinto M, Rousset M and Haffen K, Sucrase isomaltase, a marker of fetal and malignant epithelial cells of the human colon. *Int J Cancer* **32**: 407–412, 1983.
 38. Zweibaum A, Hauri HP, Sterchi E, Chantret I, Haffen K, Bamat J and Sordat B, Immunohistological evidence obtained with monoclonal antibodies of small intestine brush border hydrolases in human colon cancers and fetal colon. *Int J Cancer* **34**: 591–598, 1984.
 39. Grasset E, Bernareu J and Pinto M, Epithelial properties of human colonic carcinoma cell line Caco-2. *Am J Physiol* **248**: C410–C418, 1985.
 40. Bonneri M, Lo Gatto, Persin M and Durand G, Etude des propriétés acido-basiques et complexantes de l'acide (chloro-4 phénylthio) méthylène disphosphonique avec le magnésium et le calcium. *Bull Soc Chim (France)* **1**: 49–55, 1988.
 41. Madara JL and Dharmasathaphorn K, Occluding junctions structure-function relationship in a cultured epithelial monolayer. *J Cell Biol* **101**: 2124–2133, 1985.
 42. Windsor E and Crohnheim GE, Gastrointestinal absorption of heparin and synthetic heparinoids. *Nature* **190**: 263–264, 1961.
 43. Van Hoogdalem EJ, Wackwitz ATE, De Boer AG and Breimer DD, 3-Amino-1-hydroxypropylidene-1,1-diphosphonate (APD): a novel enhancer of rectal cefoxitin absorption in rats. *J Pharm Pharmacol* **41**: 339–341, 1989.
 44. Thiercelin JF, Zuiderwijk PBM, Peters PAM, Mensink CK, Necciari J, de Bruin H and Jonkman JHG, Tolerance and pharmacokinetic of Tiludronate at a multiple dose administration of 200, 400, 600 and 800 mg to healthy volunteers. *Vth World Conference on Clinical Pharmacology and Therapeutics, Yokohama, July 1992*, pp. 407.